Actin Filament Disassembly Is a Sufficient Final Trigger for Exocytosis in Nonexcitable Cells

Shmuel Muallem, Katarzyna Kwiatkowska, Xin Xu, and Helen L. Yin

Department of Physiology, The University of Texas Southwestern Medical Center, Dallas, Texas 75235-9040

Abstract. Although the actin cytoskeleton has been implicated in vesicle trafficking, docking and fusion, its site of action and relation to the Ca^{2+}-mediated activation of the docking and fusion machinery have not been elucidated. In this study, we examined the role of actin filaments in regulated exocytosis by introducing highly specific actin monomer-binding proteins, the β-thymosins or a gelsolin fragment, into streptolysin O-permeabilized pancreatic acinar cells. These proteins had stimulatory and inhibitory effects. Low concentrations elicited rapid and robust exocytosis with a profile comparable to the initial phase of regulated exocytosis, but without raising $[Ca^{2+}]$, and even when $[Ca^{2+}]$ was clamped at low levels by EGTA. No additional cofactors were required. Direct visualization and quantitation of actin filaments showed that β-thymosin, like agonists, induced actin depolymerization at the apical membrane where exocytosis occurs. Blocking actin depolymerization by phalloidin or neutralizing β-thymosin by complexing with exogenous actin prevented exocytosis. These findings show that the cortical actin network acts as a dominant negative clamp which blocks constitutive exocytosis. In addition, actin filaments also have a positive role. High concentrations of the actin depolymerizing proteins inhibited all phases of exocytosis. The inhibition overrides stimulation by agonists and all downstream effectors tested, suggesting that exocytosis cannot occur without a minimal actin cytoskeletal structure.

THE final steps of regulated exocytosis involve vesicle docking, triggering, and membrane fusion. There is now increasing evidence that regulated exocytosis employs a constitutively operating fusion machinery shared by many vesicular trafficking processes and specialized clamps to prevent fusion until the appropriate signals are received (4, 40, 41). The actin network under the plasma membrane has long been proposed as a physical barrier to granule docking because it transiently depolymerizes during exocytosis (3, 30, 42, 43). The cortical actin can therefore be considered as a part of the clamping apparatus. However, in many cell types, drugs which depolymerize actin do not elicit exocytosis but can potentiate agonist-evoked responses (23, 25, 38). On the basis of such evidence, it was suggested that dissolution of the actin cytoskeleton is a necessary but not sufficient part of regulated exocytosis. Nevertheless, the exact role of actin in exocytosis remains unclear, since contradictory results were obtained in other cells (1) and between intact and permeabilized cells (19). Furthermore, some cells have cytochalasin-insensitive pools of actin filaments (8). A large part of the uncertainty is due to the nonspecific nature of some of the drugs, which precludes unequivocal conclusions.

In the present study, we used a different approach to examine the relation between actin depolymerization and exocytosis. We introduced two highly specific and structurally unrelated actin monomer-binding proteins, β-thymosins (Tβ10 and Tβ4) and gelsolin S1 fragment, into streptolysin O (SLO)[1]-permeabilized pancreatic acinar cells to induce actin depolymerization. The β-thymosins are functionally similar 5 kD proteins (29, 50, 52) which were recently shown to be the predominant actin monomer-binding proteins in many cells (9, 29, 46). Gelsolin is an actin filament capping and severing protein which has a sixfold repeat structure (22). Its first repeat (segment S1) is 15 kD and it binds actin monomers (21, 45, 53). β-Thymosins and gelsolin S1 depolymerize actin by sequestering actin monomers to shift the actin monomer/polymer equilibrium towards depolymerization. These specific probes were used to explore the role of actin depolymerization in regulated exocytosis under close to physiological conditions, made possible by an SLO permeabilization protocol which maintained the structural and functional polarity of cells within the acinus and preserved their agonists-responsiveness.

Our results show that the actin cytoskeleton has direct inhibitory and facilatory roles in regulated exocytosis. Limited

Address all correspondence to Dr. Helen L. Yin, Department of Physiology, The University of Texas Southwestern Medical Center, 5323 Harry Hines Blvd., Dallas, TX 75235-9040. Fax: (214) 648-8685.

Abbreviations used in this paper: CCK, cholecystokinin; IP_3, inositol 1,4,5-triphosphate; SLO, streptolysin O; TG, Thapsigargin; TPA, phorbol 12-myristate β acetate.

actin depolymerization by the actin monomer binding proteins triggers rapid exocytosis without requiring additional cofactors, and is the basis for agonist-elicited exocytosis. Blocking actin depolymerization prevented exocytosis. Therefore, actin filaments act as a clamp to prevent constitutive exocytosis. On the other hand, extensive actin depolymerization by the monomer-binding proteins inhibits exocytosis. This inhibition overrides stimulation by agonists and all downstream effectors tested, suggesting that although exocytosis requires actin depolymerization, it cannot occur without a minimal actin structure.

Materials and Methods

Preparation of Acini and Cell Permeabilization

Rat pancreatic acini were prepared by a minimal collagenase digestion protocol (35) and resuspended in a solution containing 140 mM NaCl, 5 mM KCl, 1 mM $MgCl_2$, 1 mM $CaCl_2$, 10 mM Hepes (pH 7.4 with NaOH), 10 mM glucose, 10 mM pyruvate, 0.02% soybean trypsin inhibitor and 0.1% bovine serum albumin. The acini were kept on ice until use. Before each permeabilization experiment, ~100 mg (wet weight) of acini were washed twice in a Chelex 100-treated solution containing 140 mM KCl and 10 mM Hepes (pH 7.4), resuspended in 0.5 ml of the same buffer at 37°C containing 3 mM ATP, 5 mM $MgCl_2$, 10 mM creatinine phosphate, 5 U/ml creatinine phosphokinase, 10 μM antimycin A, 10 μM oligomycin, and 0.4 U/ml SLO (permeabilization medium). Within 1 min incubation at 37°C, more than 95% of the acini were permeabilized to heparin sulfate (4–6 kD).

Preparation of Actin-binding Proteins and Actin

Tβ4, Tβ10, and gelsolin S1, expressed in *E. coli*, were isolated as described (52, 53). The final products were >99% pure, based on Coomassie blue staining of protein bands in sodium dodecyl sulfate polyacrylamide gels. Tβ4 and Tβ10 concentrations were determined by amino acid analysis, and gelsolin S1 concentration was determined by the method of Bradford (5). Rabbit skeletal muscle Ca^{2+}-actin was converted to Mg^{2+}-actin by adding 0.2 mM EGTA and 0.4 mM $MgCl_2$ (39) polymerized, recovered by high speed centrifugation, and depolymerized by dialyzing extensively against G-actin buffer with 2 mM Tris-HCl, pH 7.8, 0.05 mM $MgCl_2$, 0.5 mM ATP, 0.1 mM dithiothreitol. Tβ10:actin complexes were formed by incubating 4 μl 100 μM Tβ10 with 3 μl 667 μM G-actin at 4°C (Tβ10:actin molar ratio of 1:5) for >1 h before addition to 200-μl cells.

Measurement of Ca^{2+} Release

The acini were permeabilized in fluorimeter cuvettes in the presence of 1 μM Fluo 3 and agonists were added with continuous stirring. Fluo 3 fluorescence was determined at excitation and emission wavelengths of 480 and 530 nm, respectively. $[Ca^{2+}]$ was calibrated by the addition of 1 mM $CaCl_2$, and then 10 mM EGTA (pH 8.5) to obtain Fmax and Fmin, respectively, and assuming a K_dCa^{2+} of 370 nM as described previously (27).

Exocytosis

Exocytosis was quantitated by measuring amylase release. Permeabilized acini (1 min SLO treatment at 37°C) were placed in an ice-cold water bath for an additional 8 min and aliquoted into 200–500-μl samples. The acini were warmed to 37°C for 2 min (defined as time 0) before stimulation with agonists or other compounds. In the case of stimulation with Ca^{2+} (Fig. 3), the permeabilized cells were diluted 1:1 into permeabilization medium containing 4 mM EGTA and different concentrations of $CaCl_2$ to give the indicated free $[Ca^{2+}]$. Final Ca^{2+} concentrations were calculated and/or measured as described (55). For time course measurements, duplicate or triplicate 50-μl samples were removed and centrifuged for 5 s at 3,000 *g*. Amylase content in the supernatants was determined (35) and expressed as percent of total before stimulation. Data shown were mean ± SEM. The cold incubation step was included to allow preincubation of cells with test substances. The SLO-induced pores did not close substantially on cooling, based on the finding that actin continued to leak out of the cells on ice. The 2-min rewarming was required to reduce $[Ca^{2+}]$ to levels found in resting cells (by uptake into intracellular stores).

Phalloidin Staining of Actin Filaments in Cells

Intact or SLO-permeabilized acini were stimulated for 5 min at 37°C, fixed in 4% paraformaldehyde in PHEM buffer (60 mM Pipes, 25 mM Hepes, 10 mM EGTA, 4 mM $MgCl_2$, pH 7.7) for 30 min and centrifuged onto poly-L-lysine-coated coverslips. Adherent cells were treated with a graded series of ice cold acetone (50/100/50% for 2, 5, and 2 min, respectively), blocked with 1% BSA in PHEM for 10 min and labeled with 0.7 μM TRITC-phalloidin (from a 70-μM stock in methanol) for 1 h at room temperature. After washing with PHEM buffer, samples were mounted in Moviol and examined with a laser scanning confocal microscope (MRC-600, BioRad Labs., Hercules, CA) with a 40×, 1.3 numerical aperture Nikon oil immersion lens. Phalloidin-stained cells were illuminated with the 488-nm line of an argon laser. Optical sections were collected and stored for later analysis. Images on the computer monitor were photographed with Kodak TMAX 100 film.

In some cases, permeabilized cells were pretreated with 5–10 μM TRITC-phalloidin before stimulation. To avoid adding large volumes of carrier solvent, stock phalloidin in methanol was evaporated under a stream of N_2, and dissolved in buffer immediately before addition to cells.

Quantitation of Actin Filament Content

Actin filament content was determined by binding to TRITC-phalloidin, which interacts with actin filaments but not actin monomers. Two methods were used for quantitation: (*1*) measurement of actin filament content in the apical plasmalemmal area by fluorescence microscopy. Confocal images of TRITC-phalloidin stained resting and stimulated pancreatic acini, collected under identical optical conditions (constant gain and background correction) were analyzed by the COMOS microscope operating system. In most cases, neutral density filter no. 1 (10% incident light) was used. In cells pretreated with high concentrations of TRITC-phalloidin, neutral density filter no. 2 (3% incident light intensity) was used to compensate for the brighter fluorescence. Control experiments showed that the fluorescence intensity of the samples were within the linear range. Images of acinar clusters (3–8 clusters per condition) were randomized and analyzed in a double blind fashion. Each image projected on the screen encompassed 768 × 512 pixels (working image magnified to 77 μm wide). An area spanning the middle of the apical membrane and covering approximately half of the length of the apical membrane of each cell and a small amount of the adjoining cortical cytoplasm was delineated (~7 × 80 pixels) and the mean fluorescence intensity determined. 13–49 cells from multiple acini and several experiments were analyzed per condition. Cells were excluded from analysis if their apical membrane was not entirely in the same plane of focus or overlapped with other cells; (*2*) bulk actin filament measurements. SLO-permeabilized cells were fixed with 4% paraformaldehyde in PBS containing 2 mM $MgCl_2$ and 3 mM EGTA, washed and incubated with 50 mM NH_4Cl in PBS for 10 min. They were permeabilized with 0.1% Triton X-100 and labeled with 0.7 μM TRITC-phalloidin (Sigma Chem. Co., St. Louis, MO) for 1 h at room temperature. Bound phalloidin was extracted with methanol. Fluorescence was measured at excitation/emission wavelengths of 540/570 nm (15). Nonspecific binding was determined by adding 10-fold excess unlabeled phalloidin and was less than 5% of total binding. The assay was within the linear range of the binding curve, determined by varying the concentration of cells used. Experiments were performed in duplicate.

Quantitative Western Blotting

Pancreatic acinar cell extracts were prepared by adding hot 3% SDS, 150 mM NaCl, 5 mM EDTA, 5 mM EGTA and 20 mM Tris, pH 7.6, to cells. Samples were boiled and disrupted by passing through 25-gauge needles. Aliquots were used for protein determination by the bichinoic acid procedure (Pierce Chemical Co., Rockford, IL) and electrophoresis in SDS-polyacrylamide gels. Western blotting was performed with monospecific antibodies as described in references 50 and 52. Purified recombinant Tβ4, muscle skeletal actin, and bovine spleen profilin were used as standards. Immunoreactive bands were visualized with the Enhanced Chemiluminescence (ECL) detection system (Amersham Corp., Arlington Heights, IL) and scanned with a 300A computing densitometer (Molecular Dynamics, Sunnyvale, CA). Values within the linear range of the protein standard curves were used to estimate the concentration of each protein in the cell lysates.

Polyclonal antibodies to β-thymosins were produced by immunizing rabbits with Tβ4. This antibody recognized Tβ4 and Tβ10, and probably most other β-thymosin isoforms because of their high sequence homology.

Monoclonal anti-actin (C4) was purchased from Boehringer Mannheim Corp. (Indianapolis, IN), and polyclonal anti-profilin was made in this laboratory.

The concentration of unpolymerized actin was estimated using the equation $[PA]=([Pt][Cc])/([Cc]+K_d)$ (12), where $[PA]$ is the concentration of binding protein:monomer complex, $[Pt]$ is the total monomer-binding protein concentration, K_d is the equilibrium constant for monomeric actin, and Cc is the critical concentration for actin polymerization. Using K_d values of 0.6 μM (46) and 1 μM (14) for binding of β-thymosins and profilin to cytoplasmic actin, respectively, and Cc of 0.5 μM (barbed ends capped), the unpolymerized actin pool under resting conditions is 0.83 μM (Cc = 0.5 μM; β-thymosin:actin = 0.14 μM; profilin:actin = 0.19 μM).

Results

Agonist-Responsiveness of the SLO-Permeabilized Cell System

SLO, a bacterial toxin, has been used by several investigators to study exocytosis in pancreatic acinar cells (see for example [34]). In all previous reports exocytosis was triggered by clamping Ca^{2+} at high concentrations or by adding various cofactors (16, 18), and not with agonists such as carbachol or cholecystokinin (CCK). In this study, we optimized the SLO permeabilization protocol to preserve agonist signaling competence and its coupling to the exocytotic machinery.

The agonist and cofactor responsiveness of the SLO-permeabilized cell system was demonstrated by their effects on Ca^{2+} release from internal stores and exocytosis. When SLO-permeabilized cells were allowed to control ambient $[Ca^{2+}]$ by Ca^{2+} uptake into internal stores, they responded to carbachol or the octapeptide CCK8 by releasing stored Ca^{2+}. This increased $[Ca^{2+}]$ to ~400 nM ($n > 70$) (Fig. 1, *a* and *b*), a level comparable to that observed in intact cells (28). The permeabilized cells also responded to the membrane impermeant GTPγS (*c*) which activates the G-protein signaling pathways, and to inositol 1,4,5-trisphosphate (IP_3) (*e*) which directly activates the Ca^{2+} release channels. Thapsigargin (TG), an inhibitor of intracellular store Ca^{2+} pumps, induced a slower, sustained rise in $[Ca^{2+}]$ (*d*).

Cells permeabilized in the absence of actin depolymerizing proteins retained an intact exocytotic apparatus. Exocytosis was quantitated by measuring amylase secretion after fusion of zymogen granules with the plasma membrane. Basal release was low, indicating that there was minimal granule lysis by SLO. CCK8 induced a biphasic exocytotic response (Fig. 2 *A*) with a short, rapid phase and a sustained, slower phase. The robust responses to several downstream effectors were entirely consistent with the pattern in intact cells (35). Thus, GTPγS stimulated the highest level of secretion (Fig. 2 *A*), probably due to the combined activation of multiple G-proteins, including those in the PLC pathway used by CCK8 or carbachol, and the cAMP-dependent pathway. IP_3 and TG stimulated release mostly during the initial 5 min, while phorbol 12-myristate 13 acetate (TPA) elicited secretion at a prolonged phase (Fig. 2 *B*).

Effects of Actin Monomer-binding Proteins on Exocytosis

Unexpectedly, 1 μM Tβ10 stimulated amylase release in the absence of agonists (Fig. 2 *A*). Its effect on the initial phase of release was particularly striking; amylase was secreted more rapidly than after stimulation with optimal concentrations of CCK8 or its downstream effectors. In four separate experiments, the initial rates of amylase release in response to CCK8 or 1 μM Tβ10 were 1.37 ± 0.11% and 1.91 ± 0.18% of total amylase/min, respectively. The rapid time course and robust response suggested that the Tβ10 directly triggered an important final step in amylase release and its effects were not secondary to the inadvertent generation of second messengers. $[Ca^{2+}]$ measurements showed that 1 μM Tβ10 did not release Ca^{2+} from internal stores (Fig. 1 *f*), indicating that it did not elicit exocytosis by raising $[Ca^{2+}]$ (also see below). The small initial Ca^{2+} spike at 10 μM Tβ10 (Fig. 1 *f*) was due to a slight Ca^{2+} contamination

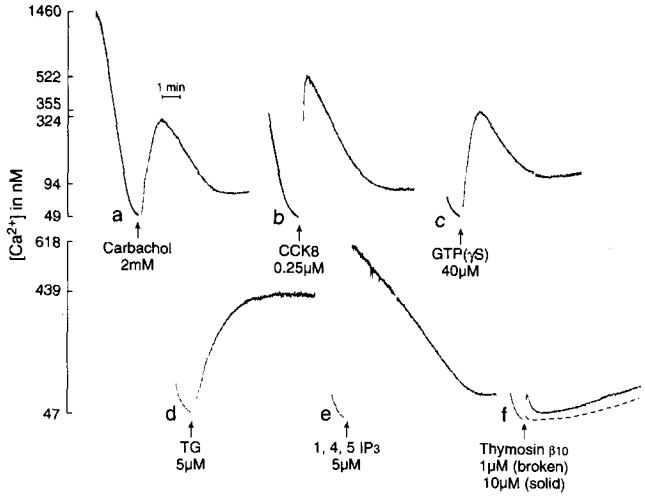

Figure 1. Ca^{2+} signaling in SLO-permeabilized pancreatic acini. $[Ca^{2+}]$ was estimated by Fluo 3 fluorescence. The acini reduced medium $[Ca^{2+}]$ to ~50 nM by uptake into internal stores. Stimuli at the final concentrations shown in the figure were added at time 0 as indicated by arrows.

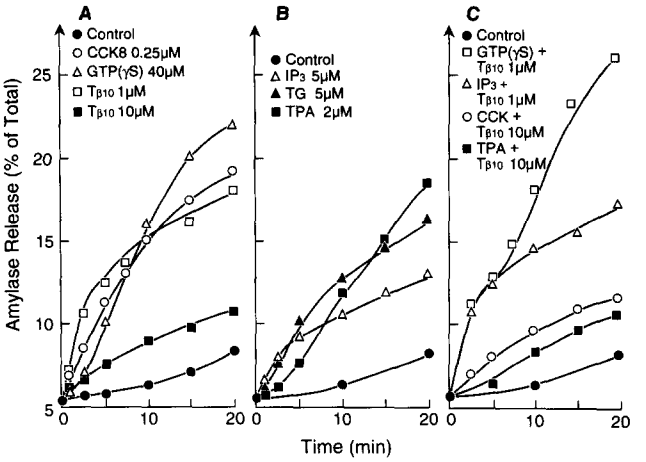

Figure 2. Exocytosis by SLO-permeabilized acini. Acini were permeabilized and exocytosis was measured as described in Materials and Methods (*A–C*). Time course of exocytosis. Control was without added stimulus. Tβ10 was added 1 min after exposure to SLO at 37°C. Cells were incubated for 8 min at 4°C and warmed for 2 min before addition of agonists/effectors (defined as time 0 in graph). Data shown are averages of triplicates and are representative of 3–5 different experiments.

in the Tβ10 sample which was rapidly sequestered into the intracellular stores. Tβ10 did not stimulate amylase release from nonpermeabilized cells (data not shown), demonstrating that its site of action was inside the cell.

To evaluate if Tβ10 stimulated exocytosis by the same mechanism as agonists, permeabilized cells treated with 1 μM Tβ10 were challenged with agonists or downstream effectors. 5 μM IP_3 did not enhance secretion above the level observed with Tβ10 alone (Fig. 2 *A*). A similar lack of additivity was observed with TG (data not shown). Therefore, Tβ10, IP_3 and TG appeared to elicit the rapid exocytosis of a pool of secretory granules by a common mechanism. Likewise, GTPγS (Fig. 2 *C*), CCK8, or TPA (not shown) did not stimulate the initial phase of exocytosis beyond that observed with Tβ10 alone. GTPγS however potentiated the Tβ10 effect during prolonged stimulation periods (Fig. 2 *C*), suggesting that they have nonoverlapping actions at some steps in the cascade.

Due to the prominent role of Ca^{2+} in exocytosis, we tested the effect of Tβ10 while clamping [Ca^{2+}] with EGTA during cell stimulation. Fig. 3 shows that increasing medium [Ca^{2+}] was sufficient to trigger exocytosis. The apparent affinity for Ca^{2+} was ~4.7 ± 0.8 μM (n = 3), which is within the range reported previously under similar conditions (16, 17). In the presence of 2 nM Ca^{2+} (2 mM EGTA and no added $CaCl_2$), 1 μM Tβ10 increased the rate of exocytosis by more than 50%. Between 0.1 and 1 μM Ca^{2+}, the Tβ10 elicited exocytosis had a shallow and minimal dependence on [Ca^{2+}]. The reduced effectiveness of Tβ10 at high EGTA and no added Ca^{2+} probably was due to non-specific perturbations by EGTA, since all forms of stimulated secretion were similarly affected. Hence, it appears that Tβ10-elicitated exocytosis is predominantly Ca^{2+}-independent. This is expected from the fact that actin depolarization by Tβ10 is independent of Ca^{2+} and indicates that Tβ10 acts at a step coincidental or distal to that affected by Ca^{2+}.

Since the only known intracellular function of Tβ10 is to sequester actin monomers, the most straightforward interpretation of our result is that Tβ10 stimulated exocytosis by depolymerizing actin filaments. It therefore follows that other actin depolymerizing proteins which are small enough to penetrate the SLO-permeabilized membrane pores should also induce secretion. This was indeed the case. Tβ4, a functionally identical thymosin isoform (50, 52), had similar effects as Tβ10 (data not shown). Gelsolin S1, which binds actin monomer but is structurally distinct from the β-thymosins, stimulated exocytosis at a low concentration (Fig. 4 *B*). The common action of the structurally unrelated classes of actin depolymerizing proteins provided strong evidence for their action through actin depolymerization. It should also be pointed out that neither β-thymosin nor gelsolin has amphipathic structures which may act as fusogens to promote membrane fusion (26, 54).

Biphasic Effects of Actin Monomer-binding Proteins

Titration of Tβ10 and gelsolin S1 showed that they had biphasic effects on exocytosis. Tβ10 concentrations of up to 2 μM stimulated, whereas higher concentrations inhibited exocytosis (Fig. 2 *A* and 4 *A*). Gelsolin S1 likewise had stimulatory and inhibitory effects (Fig. 4 *B*). In the remainder of the paper, we will present additional data using

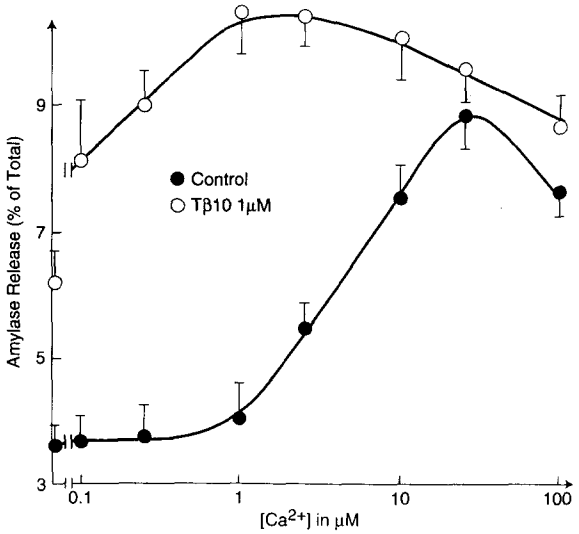

Figure 3. Simulation of exocytosis at defined [Ca^{2+}]. Acini were permeabilized and diluted into media with defined [Ca^{2+}] as described in Materials and Methods. Tβ10 was added during the cold incubation and also included in the EGTA-containing dilution media. 5 min after dilution to start the experiments, samples were removed to measure amylase. [Ca^{2+}] at the far left of the x-axis is 2 nM. Data show the mean ± SEM of three experiments performed in duplicates.

Tβ10 because of its small size, simple interaction with actin, insensitivity to second messengers and lack of known post-translational modifications (29, 52).

Tβ10 was not only self-inhibitory, it also inhibited release in response to CCK8, TPA (Fig. 2 *C*), carbachol (Fig. 4 *A*), IP_3, and TG (data not shown). Since some of these stimuli act at distinct steps in converging signaling cascades, the universal inhibitory effect of Tβ10 was consistent with the disruption of a critical downstream event required for exocytosis. Tβ10 inhibition was not due to nonspecific cell damage; the cells were able to generate Ca^{2+} transients in response to agonists and IP_3 (data not shown).

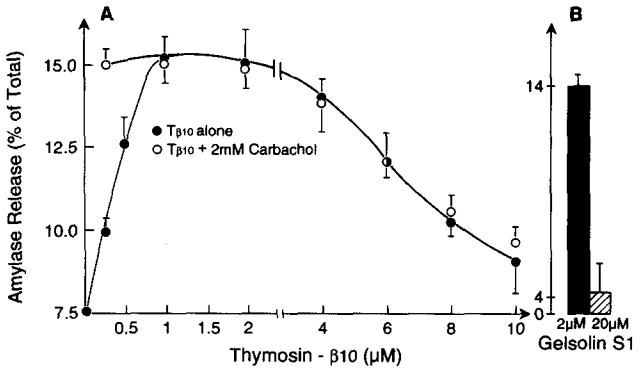

Figure 4. Biphasic effects of Tβ10 and gelsolin S1 on exocytosis. Acinar cells were permeabilized and treated with Tβ10 or gelsolin S1 as described in Materials and Methods. Amylase release in the supernatant was measured 10 min after the start of incubation at 37°C. Values shown were average ± SEM (n = 3). *A*, Tβ10, with and without 2 × 10^{-3} M carbachol. *B*, gelsolin S1.

Effects of Agonists or Tβ10 on the Actin Cytoskeleton

Tetramethyl rhodamine isothiocyanate (TRITC)-phalloidin was used to visualize actin filament organization in cells. Intact cells had a thick actin rim at the apical and upper lateral surfaces and faint staining at the basal membrane. Some diffuse staining was observed in the cytoplasm (Fig. 5 *A*). Cells treated with 10^{-9} M CCK8 (which stimulated exocytosis) for 5 min had significant actin filament loss which was particularly striking at the apical and lateral membranes (Fig. 5 *B*). Since pancreatic acinar cell secrete exclusively from their apical surface, these images demonstrated a loss of actin filament structures at the site of exocytosis. There was a marked increase in the width of the lumens which may be attributed to vectorial secretion and accumulation of fluid, electrolytes, and secretory products after exocytosis.

Unstimulated SLO-permeabilized cells had a similar actin-staining pattern as intact cells, except that the basal subplasmalemmal actin staining was fainter (Fig. 6 *A*). Agonist at a concentration which elicited exocytosis again reduced apical and lateral staining (Fig. 6 *B*). Remarkably there was also considerable expansion of the luminal spaces, suggesting that the tight junctions and apical membranes were sufficiently intact to allow vectorial exocytosis and fluid secretion even after SLO treatment. Higher magnification images show that the apical actin rim had decreased staining intensity and appeared to be wavy, compared with control cells (Fig. 6, *B'* and *A'*, respectively).

2 μM Tβ10, which stimulated exocytosis, likewise decreased actin staining and promoted luminal expansion (Fig. 6, *C* and *C'*). Therefore, limited actin depolymerization by Tβ10 caused the same structural changes as agonist stimulation, including membrane expansion and generation of luminal spaces, which are indicative of robust exocytosis.

20 μM Tβ10, which inhibited exocytosis, further reduced actin staining (data not shown). The apical spaces were not expanded, as would be consistent with the absence of exocytosis. Although actin staining was significantly reduced with an inhibitory concentration of Tβ10, the pattern of actin loss was not qualitatively different from that obtained with a stimulatory concentration. Therefore, it was not possible to determine at this resolution whether the same or different populations of actin filaments were involved.

Effects on Actin Filament Content

A decrease in actin filament content during agonist or Tβ10-induced exocytosis was substantiated by direct quantitation of TRITC-phalloidin staining of the apical plasma membrane and bulk actin filaments. The intensity of phalloidin staining of the apical membrane is summarized in Table I. Intact cells stimulated with CCK8 had reduced actin filament intensity (70.9% of control). SLO-permeabilized cells treated with CCK8 or 2 μM Tβ10 which stimulated exocytosis had a comparable reduction in actin filament intensity (61.6% and 66.5% of control, respectively). 20 μM Tβ10 which inhibited exocytosis reduced actin staining further to 36.2% (data not shown). These results demonstrated that Tβ10 depolymerized actin filaments at the site of exocytosis in a dose-dependent manner, and Tβ10 stimulated exocytosis is accompanied by depolymerization to an extent comparable to that observed after agonist stimulation. Depolymerization of actin by Tβ10 was consistent with its ability to sequester actin monomers in vitro and in vivo (37, 50).

A decrease in filament content was also demonstrated by a bulk fluorimetric phalloidin-binding assay. Agonist stimulation reduced total actin filament content in permeabilized cells to 84.5 ± 2.7% ($n = 4$) of control, while 2 μM Tβ10 reduced actn to 83.6 ± 4.1% ($n = 5$) of control. These estimates were 18–22% less than those based on apical actin staining, raising the possibility that there may be some preferential loss of apical actin filaments.

Effects of Blocking Actin Depolymerization

To strengthen the link between actin depolymerization and exocytosis, we tested the effect of blocking actin depolymerization by high concentrations of phalloidin (7). Pretreatment of permeabilized cells with 10 μM phalloidin inhibited CCK-induced and Tβ10-induced amylase release to 13% and 28% of control, respectively (Table II), even though phalloidin up to 25 μM had no apparent effect on CCK-induced Ca^{2+}-transients (data not shown). Inhibition of actin depolymerization and exocytosis was confirmed morphologically. Control cells which were permeabilized in the presence of 10 μM TRITC-phalloidin had bright actin staining (Fig. 6 *D*). CCK8 or Tβ10 had much less effect on actin depolymerizing and exocytosis on phalloidin-stabilized cells, as evidenced by the persistence of bright actin staining and narrow lumens (Fig. 6, *E* and *F*). Direct quantitation of apical actin intensity showed that less than 10% of apical actin was depolymerized compared with 30–40% for cells not stabilized with phalloidin (Table I). The extent of inhibition

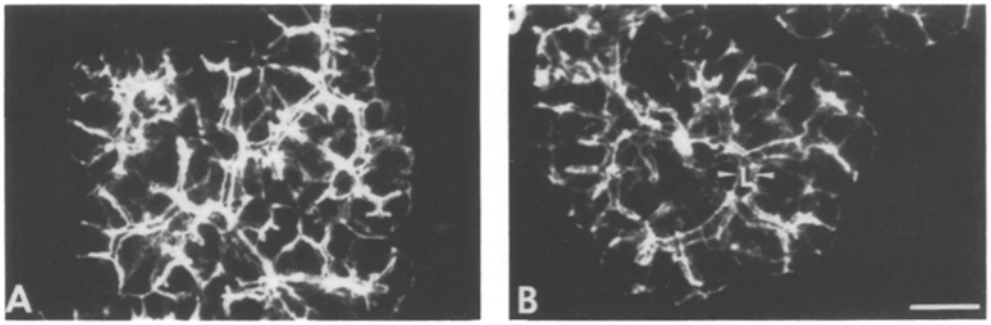

Figure 5. Actin filament distribution in intact acinar cells. Intact acini were incubated with buffer or 10^{-9} M CCK8 for 5 min, fixed, and stained with 0.7 μM TRITC-phalloidin. Samples were examined with a 40× oil immersion objective under a laser scanning confocal microscope (BioRad Labs.). *A*, buffer control; *B*, 10^{-9} M CCK8. Arrowheads indicate lumen (*L*). Bar, 25 μm.

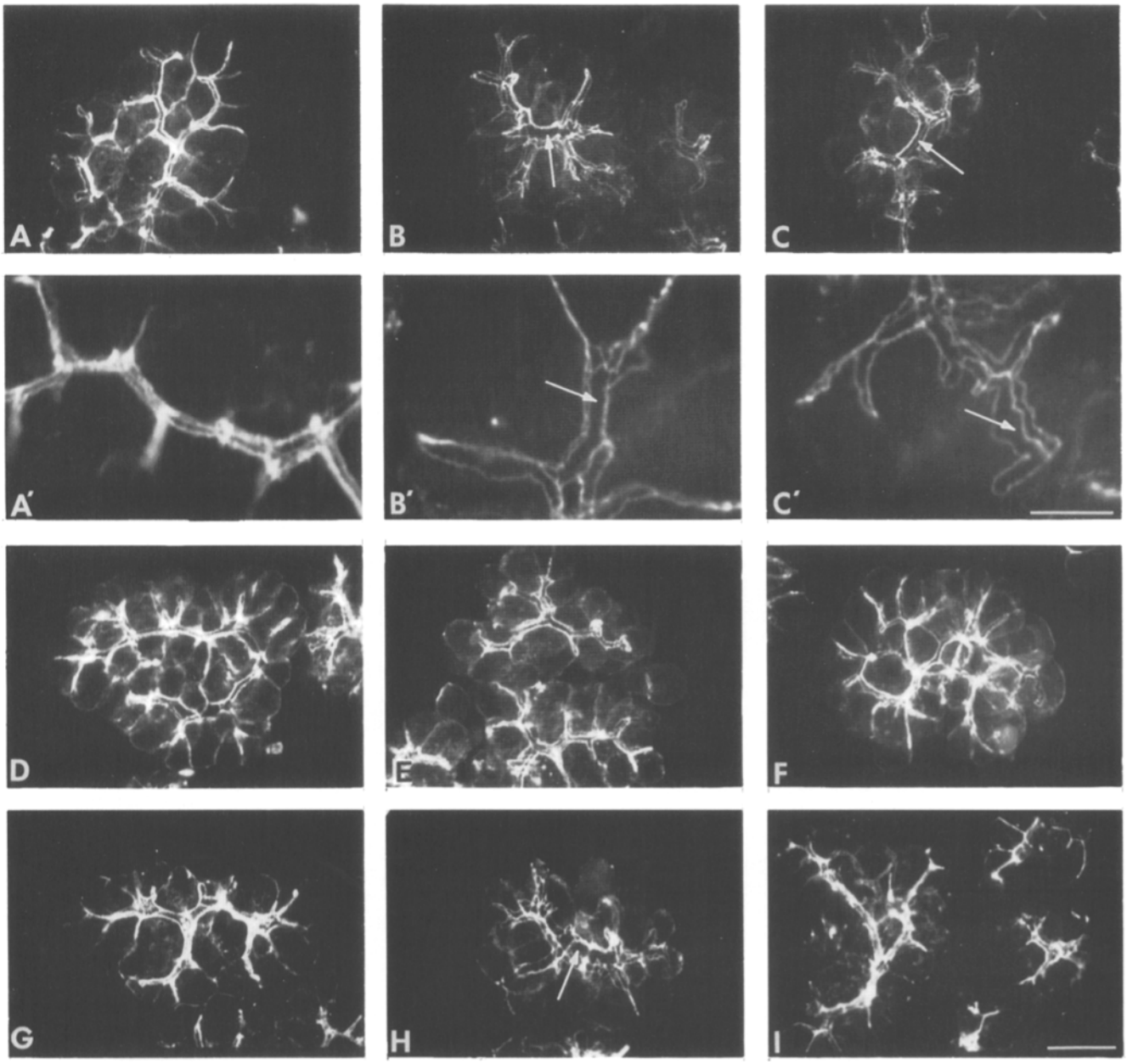

Figure 6. Actin filament distribution in SLO-permeabilized acini stimulated with CCK8 or Tβ10. The experimental conditions were identical to those described in Table I. (*A–C*) Incubated with buffer, 10^{-7} M CCK8, or 2 μM Tβ10; (*A′–C′*) conditions same as *A–C*, at higher magnifications; (*D–F*), cells pretreated with 10 μM TRITC-phalloidin, and stimulated with buffer, CCK8, or Tβ10, respectively. (*G–I*) 10 μM G-actin added at time 0, in the presence of buffer CCK8, or Tβ10. *Arrows*, expanded lumens. Bars: (*A–I*) 25 μm, (*A′–C′*) 10 μm.

of actin depolymerization was comparable to the inhibition of exocytosis (compare Tables I and II).

To further evaluate this relation, we tested the effect of inactivating Tβ10 with actin monomers before addition to cells. Since Tβ10 depolymerizes actin by binding actin monomers, Tβ10 bound to exogenous actin should be less effective in depolymerizing endogenous actin. This was indeed the case. Tβ10 preincubated with actin monomers did not cause exocytosis (Table II), actin depolymerization, and luminal expansion (Fig. 6, *G* and *I*, Table I). In contrast, 5 μM actin reduced the inhibitory effect of 10 μM Tβ10, resulting in an increase in exocytosis. We interpret this to mean that actin bound a fraction of Tβ10, reducing its effective concentration to produce a leftward shift in the Tβ10 dose response curve (similar to that shown in Fig. 4 *A*). The ability of exogenous actin to reduce/enhance Tβ10 effects is consistent with the biphasic effects of Tβ10, and confirmed that both actions are specifically related to its ability to depolymerize actin. In contrast, exogenous actin alone had little effect on CCK8-induced actin depolymerization (Fig. 6 *H*) and exocytosis (Table II). It is not clear at present why exogenous actin had no effect. The simplest explanation is that in the absence of Tβ10, exogenous actin polymerizes immediately when added to the cell medium, and the filaments

Table I. Quantitation of Apical Actin Filaments

Treatments	Stimuli*					
	Buffer		CCK8		Tβ10	
	Intensity‡		Intensity		Intensity	
		%		%		%
Intact cells:						
Buffer	152.5 ± 5.3 (n = 30)	100	108.2 ± 4.4 (n = 25)	70.9	–	–
Permeabilized cells:						
Buffer	173.6 ± 5.0 (n = 16)	100	106.9 ± 4.0 (n = 17)	61.6	115.5 ± 3.6 (n = 17)	66.5
Phalloidin§	168.1 ± 2.6 (n = 49)	100	155.6 ± 2.7 (n = 41)	92.6	151.9 ± 2.6 (n = 42)	90.4
Actin‖	198.2 ± 8.2 (n = 13)	100	–	–	199.5 ± 2.8** (n = 18)	100.8

* Intact cells were stimulated with 10^{-9} M CCK8 for 5 min at 37°C. Semi-intact cells (permeabilized with SLO for 1 min at 37°C, incubated for 8 min at 4°C and rewarmed for 2 min) were treated with 10^{-7} M CCK8 or 2 μM Tβ10 for 5 min at 37°C (higher CCK8 concentration was required to elicit maximal exocytosis in permeabilized than in intact cells). Cells were fixed with paraformaldehyde, centrifuged onto coverslips, treated with acetone, and stained with 0.7 μM TRITC-phalloidin.

‡ Apical actin filaments were quantitated by measuring fluorescence intensity in microscopic images. Cells subjected to buffer or actin treatments, and cells pretreated with phalloidin were imaged with neutral density filters no. 1 and no. 2 (to reduce incident light to 10% and 3%, respectively), at constant gain and background corrections. Data shown were mean light intensity ± SEM. n, number of cells analyzed. The differences between stimulated and unstimulated (buffer control) cells within each treatment condition were statistically significant ($p < 0.001$, based on Student's t test) in all cases except one (indicated by **).

§ TRITC-phalloidin was added to cells to a final concentration of 10 μM at 0.5 min after SLO addition. After stimulation, cells were fixed with paraformaldehyde and acetone, and stained additionally with 0.7 μM TRITC-phalloidin as above. The second staining after acetone extraction was not essential, but was included in case phalloidin was not able to label certain actin populations in the semi-intact cells.

‖ Actin (10 μM in G-actin buffer) or 10 μM actin/2 μM Tβ10 was added to cells at time 0. G-actin buffer accounted for 1.5% of the final volume and had no effect by itself.

are too big to enter the SLO-generated membrane pores. We did not investigate this and other possibilities further. The overall results in Tables I and II establish that Tβ10 elicited exocytosis by acting as an actin monomer-binding protein and ruled out other actions via unidentified contaminating effectors.

Endogenous Concentrations of Interactive Components

The marked effects observed with low concentrations of β-thymosins were initially surprising since the endogenous β-thymosin level may be high (9) and β-thymosins depolymerize actin stoichiometrically. To understand why β-thymosin was so effective in the permeabilized cell system, we estimated the concentration of actin monomer-binding proteins and actin. Fig. 7 shows Western blots of acinar extracts and purified protein standards with anti-β-thymosins (*A*) and anti-actin (*B*). The anti-β-thymosin recognized a single band in the cell lysate which comigrated with purified Tβ4. Densitometry scanning of these and other blots showed that the permeabilized cell extracts contained 0.32 ± 0.01 μM (n = 4) β-thymosins, 1.36 ± 0.08 μM (n = 4) actin, and 0.58 ± 0.03 μM (n = 5) profilin. Assuming that β-thymosins and profilin are the predominant actin monomer buffering proteins and the filaments are capped, the unpolymerized actin pool under resting conditions is 0.83 μM (calculated as described in Materials and Methods). This estimate is consistent with an approximation based on the amount of triton X soluble actin (0.76 μM, data not shown). Exogenous β-thymosin would shfit the monomer:polymer equilibrium towards depolymerization. Since the initial actin filament concentration was low, a small amount of exogenous β-thymosin causes extensive actin depolymerization in a system poised towards depolymerization.

Table II. Effect of Phalloidin and Exogenous Actin on Stimulated Exocytosis

Treatments*	Stimuli		
	CCK8	Tβ10 (1 μM)	Tβ10 (10 μM)
	%	%	%
–	100	100	19 ± 5
Phalloidin	13 ± 6	28 ± 9	–
Actin	108 ± 11	7 ± 6	44 ± 7

* Phalloidin (10 μM) or actin (5 μM in G-actin buffer) was added 30 s after permeabilization with SLO. After a cold incubation and rewarming, the cells were stimulated with 10^{-9} M CCK8 or Tβ10 for 5 min and amylase released to the incubation medium was determined. Values obtained with CCK8 or with 1 μM Tβ10 without additional treatments were defined as 100%; other values were expressed relative to them (mean ± SEM, n = 3–5 experiments).

Discussion

The pancreatic acinus is a classical model for regulated exocytosis by nonexcitable cells (13, 48). Two phases of exocytosis are proposed: an initial phase, which is completed within 5 min of cell stimulation, and a second phase which is sustained for the duration of agonist stimulation. Ample evidence showed that the first phase is mediated by an increase in $[Ca^{2+}]_i$, whereas the second phase is associated with stimulation of protein kinase C (35, 48). In analogy to neurotransmission, it is postulated that the first phase represents fusion of primed granules which are in the vicinity of the plasma membrane, while the second phase is due to release from a reserve pool.

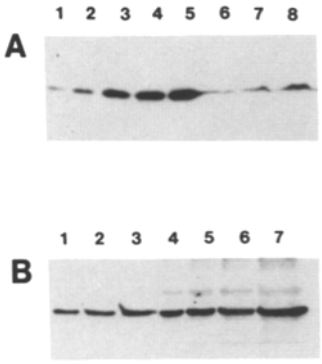

Figure 7. Quantitation of β-thymosin and actin content. (*A*). Immunoblotting with anti-β-thymosin. (Lanes *1–5*) Purified recombinant Tβ4 at 10, 20, 40, 50, and 75 ng. (Lanes *6–8*) Acinar cell extracts at 60, 84, and 120 μg. In the experiment shown, β-thymosin, estimated by calibration against the linear portion of the Tβ4 standard curve, accounted for 0.02% of total protein (equivalent to 0.4 μM in a SLO-permeabilized cell extract). (*B*) Immunoblotting with anti-actin. (Lanes *1–3*) 12, 24, and 45 ng purified rabbit skeletal muscle actin. (Lanes *4–7*) 5, 10, 20, and 40 μg extracts. Actin accounted for 0.6% of total protein (equivalent to 1.4 μM in a permeabilized cell extract).

The SLO-permeabilized cell system used in the present studies retained the major features of this exocytotic machinery and its regulation. Accordingly, agonist stimulation and GTPγS triggered exocytosis over long periods of time, IP_3 and TG elicited Ca^{2+} increase to activate a short lasting phase, and TPA affected exocytosis after a lag and at constant, low $[Ca^{2+}]$. Because of the preservation of these universal and well-characterized stimulus-secretion coupling responses, the SLO-permeabilized acinar system permitted a careful dissection of the role of the actin cytoskeleton under close to physiological conditions.

Our results show that actin filaments have direct inhibitory and facilitory roles in regulated exocytosis; limited depolymerization of actin filaments is a sufficient final trigger for regulated exocytosis, and further actin depolymerization blocks exocytosis.

Triggering Exocytosis by Actin Filament Depolymerization

The actin network under the plasma membrane has been proposed as a physical barrier to granule docking because it transiently depolymerizes before exocytosis in a variety of cells (3, 42, 43). However, O'Kinski and Pandol (32, 33) reported that a CCK analog did not cause actin depolymerization at concentrations which stimulated exocytosis, but CCK8 caused actin depolymerization at supramaximal concentrations which inhibited exocytosis. Our results using intact and permeabilized cells clearly showed that actin depolymerization was associated with CCK8 stimulation of exocytosis. This relation was further supported by the ability of low concentrations of Tβ10 to elicit exocytosis.

Several observations indicate that Tβ10 elicited exocytosis by acting as an actin monomer-binding protein. They include: (*a*) no effect on intact cells; (*b*) all actin depolymerizing proteins tested stimulate exocytosis in permeabilized cells; (*c*) stimulatory concentrations of Tβ10 and agonists produced similar patterns of actin depolymerization and exocytosis; (*d*) Tβ10 did not mobilize Ca^{2+}; (*e*) Tβ10 stimulated exocytosis even when $[Ca^{2+}]$ was clamped at low levels with EGTA; (*f*) Tβ10 effects were blocked by exogenous actin or phalloidin; (*g*) feasibility of the actin depolymerization model based on the concentrations of interactive components. The stimulatory effect of Tβ10 was due to partial breakdown of the actin barrier at the site of exocytosis. The rate and extent of exocytosis were comparable to the initial phase of exocytosis induced by agonists. Furthermore, agonists did not potentiate the stimulatory effect of Tβ10. Therefore, selective actin depolymerization has a primary role in the agonist-evoked exocytosis. Our conclusion does not preclude a role of agonists in regulating other events in the secretory pathway; the additivity of Tβ10 and GTPγS effects after prolonged incubation suggests that further modulations are possible, as has been proposed for other secretory systems (30, 41).

All conventional mediators of the rapid phase of exocytosis (agonists, GTPγS, IP_3, and TG) increased the $[Ca^{2+}]$ of the incubation medium. In contrast, Tβ10 triggered rapid exocytosis without changing $[Ca^{2+}]$ and even when $[Ca^{2+}]$ was clamped at low levels. Furthermore, a $[Ca^{2+}]$ increase caused by any one of the Ca^{2+}-mobilizing agents had no additive effect on the Tβ10 induced exocytotic response. Hence, actin depolymerization by Tβ10 bypassed the need for a large increase in $[Ca^{2+}]$. It follows that one of the major consequences of the agonist-induced $[Ca^{2+}]_i$ increase in intact acinar cells, may be actin depolymerization at the site of exocytosis. This can be mediated by Ca^{2+}-dependent filament severing/capping actin regulatory proteins such as gelsolin, scinderin and CapG (43, 49, 51), or by other Ca^{2+} sensors, such as synaptotagmin (11, 36), and p145/CAPS (24, 44) which can potentially modulate the actin cytoskeleton indirectly.

Existence of an Actin Clamp for Exocytosis

The finding that actin depolymerization per se causes exocytosis in the acinar cells has profound implications for the underlying molecular mechanisms of granule docking, fusion, and content release. It implies that a substantial portion of the granule and plasma membranes are fusion competent, provided that the actin barrier is removed. This is consistent with the prevailing hypothesis that cells have a constitutive fusion machinery which is clamped to prevent fusion, until an appropriate activation signal is received (4, 40, 41). In pancreatic acinar cells, the actin network at the site of exocytosis acts as a dominant negative clamp for regulated exocytosis.

The actin clamp is likely to exist in other cell types. However, since cytochalasin which also depolymerizes actin filaments does not trigger exocytosis in neutrophils and neuroendocrine cells (23, 31, 38), other clamps may also be in place. Synaptotagmin is a currently favored candidate for such a clamp in neuronal cells (36). Nevertheless, the discovery that synaptotagmin null or loss-of-function mutants have a range of phenotypes and are, in most cases, still capable of regulated exocytosis (for review see reference 36) is consistent with the existence of multiple clamping mechanisms. In the context of the findings presented here, it would appear that even after elimination of the synaptotagmin clamp, the actin clamp remains intact and has to be released by appropriate stimuli. Since there are suggestions that synaptotagmin modulates the actin cytoskeleton (11), it will be important to determine if the sequential clamps act independently or are coupled and interactive.

A Minimal Actin Machinery Is Required for Exocytosis

Although exocytosis requires actin depolymerization, it cannot occur without a minimal actin structure. Therefore, actin

filaments have a positive, in addition to a negative, role in regulated exocytosis. The positive role is demonstrated by the ability of high concentrations of Tβ10, which cause extensive actin depolymerization, to inhibit exocytosis and prevent stimulation by all effectors. The comprehensive inhibition of exocytosis suggests that actin filaments are required for completion of a step close to or downstream of granule docking at the plasma membrane. To the best of our knowledge, this is the first direct demonstration of inhibition of exocytosis by actin depolymerization at a late step of exocytosis. This can explain the inhibition of pancreatic enzyme secretion by high concentrations of cytochalasin B reported almost two decades ago (2). Previous studies in pancreatic acinar and other cell types have suggested that intact actin filaments are required for earlier steps such as granule transport to the site of exocytosis (2, 6, 10, 20, 47). Inhibition of exocytosis by extensive actin depolymerization was also observed after treatment with supramaximal agonist concentrations which inhibit exocytosis (32, 33). The remarkably similar appearance of the actin cytoskeleton in cells treated with inhibitory concentrations of Tβ10 and agonists suggest a common mechanism of inhibition. It is not clear at present whether the inhibitory and facilatory actin filaments represent different pools which are differentially sensitive to the depolymerizing action of the β-thymosins and gelsolin.

The direct relation between actin depolymerization and exocytosis found in the acinar cells makes them a particularly attractive model to study how agonists induce actin depolymerization to elicit exocytosis and why a minimal actin structure is required for regulated exocytosis. The use of highly specific actin modulatory proteins permits the molecular dissection of the membrane-cytoskeletal linkages between the very early and late events in regulated exocytosis.

We thank Mahrooz Khademazed for expert technical assistance.

This work is supported by National Institutes of Health (NIH) grants NS31430 and GM51112, The Welch Foundation (to H. L. Yin), and NIH grants DK32938 and DK46591 (to S. Muallem).

Received for publication 10 August 1994 and in revised form 29 September 1994.

References

1. Bader, M.-F. A. G. Garcia, J. Ciesielski-Treska, D. Thierse, and D. Aunis. 1983. Contractile proteins in chromaffin cells. *Prog. Brain Res.* 58:21-29.
2. Bauduin, H., C. Stock, D. Vincent and J. F. Grenier. 1975. Microfilamentous system and secretion of enzyme in the exocrine pancreas. *J. Cell Biol.* 66:165-181.
3. Bengtsson, T., C. Dahlgren, O. Stendahl, and T. Andersson. 1991. Actin assembly and regulation of neutrophil function: effects of cytochalasin B and tetracaine on chemotactic peptide-induced O_2-production and degranulation. *J. Leukocyte Biol.* 49:236-244.
4. Bennett, M. K., and R. H. Scheller. 1993. The molecular machinery for secretion is conserved from yeast to neurons. *Proc. Natl. Acad. Sci. USA.* 90:2559-2563.
5. Bradford, M. M. 1976. A rapid and sensitive method for the quantitation of microgram quantities of protein utilizing the principle of protein-dye binding. *Annu. Rev. Biochem.* 72:248-254.
6. Brady, S., R. Lasek, R. D. Allen, H. L. Yin, and T. P. Stossel. 1984. Gelsolin inhibition of axonal transport indicates a requirement for microfilaments. *Nature (Lond.).* 310:56-58.
7. Cano, M. L., L. Cassimeris, M. Joyce, and S. H. Zigmond. 1992. Characterization of tetramethylrhodaminyl-phalloidin binding to cellular F-actin. *Cell Motil. Cytoskeleton.* 21:147-158.
8. Cassimeris, L., H. McNeill, and S. H. Zigmond. 1990. Chemoattractant-stimulated polymorphonuclear leukocytes contain two populations of actin filaments that differ in their spatial distributions and relative stabilities. *J. Cell Biol.* 110:1067-1075.
9. Cassimeris, L., D. Safer, V. T. Nachmias, and S. H. Zigmond. 1992. Thymosin β4 sequesters the majority of G-actin in resting human polymorphonuclear leukocytes. *J. Cell Biol.* 119:1261-1270.
10. Fath, K. R., and D. R. Burgess. 1993. Golgi-derived vesicles from developing epithelial cells bind actin filaments and possess myosin-I as a cytoplasmically oriented peripheral membrane protein. *J. Cell Biol.* 120:117-127.
11. Feany, M. B., and K. M. Buckley. 1993. The synaptic vesicle protein synaptotagmin promotes formation of filopodia in fibroblasts. *Nature (Lond.).* 364:537-540.
12. Fechheimer, M., and S. H. Zigmond. 1993. Focusing on unpolymerized actin. *J. Cell Biol.* 123:1-5.
13. Gardner, J. D., and R. T. Jensen. 1986. Receptors and cell activation associated with pancreatic enzyme secretion. *Annu. Rev. Physiol.* 48:103-117.
14. Goldschmidt-Clermont, P. J., L. M. Machesky, S. K. Doberstein, and T. D. Pollard. 1991. Mechanism of the interaction of human platelet profilin with actin. *J. Cell Biol.* 113:1081-1089.
15. Howard, T. H., and C. O. Oresajo. 1985. The kinetics of chemotactic peptide-induced change in F-actin content, F-actin distribution, and the shape of neutrophils. *J. Cell Biol.* 101:1078-1085.
16. Jena, B. P., P. J. Padfield, T. S. Ingebritsen, and J. D. Jamieson. 1991. Protein tyrosine phosphatase stimulates Ca^{2+}-dependent amylase secretion from pancreatic acini. *J. Biol. Chem.* 26:17744-17746.
17. Kitagawa, M., J. A. Williams, and R. C. De Lisle. 1990. Amylase release from streptolysin O-permeabilized pancreatic acid. *Am. Physiol. Soc.* 259:G157-G164.
18. Kitagawa, M., J. A. Williams, and R. C De Lisle. 1991. Interactions of intracellular mediators of amylase secretion in permeabilized pancreatic acini. *Biochim. Biophys. Acta.* 107:129-135.
19. Koffer, A., P. E. R. Tatham, and B. D. Gomperts. 1990. Changes in the state of actin during the exocytotic reaction of permeabilized rat mast cells. *J. Cell Biol.* 111:919-927.
20. Kuznetsov, S. A., G. M. Langford, and D. G. Weiss. 1992. Actin-dependent organelle movement in squid axoplasm. *Nature (Lond.).* 356:722-725.
21. Kwiatkowski, D., P. A. Janmey, J. Mole, and H. L. Yin. 1985. Isolation and properties of two actin-binding domains in gelsolin. *J. Biol. Chem.* 260:15232-15238.
22. Kwiatkowski, D. P., T. P. Stossel, S. H. Orkin, J. E. Mole, H. R. Colten, and H. L. Yin. 1986. Plasma and cytoplasmic gelsolins contain a duplicated actin-binding domain. *Nature (Lond.).* 323:455-458.
23. Lelkes, P. I., J. E. Friedman, K. Rosenheck, and A. Oplatka. 1986. Destabilization of actin filaments as a requirement for the secretion of catecholamines from permeabilized chromaffin cells. *FEBS (Fed. Eur. Biochem. Soc.) Lett.* 208:357-363.
24. Martin, T. F. J. 1994. Identification of proteins required for Ca^{2+}-activated secretion. *Ann. NY Acad. Sci.* 710:328-332.
25. Matter, K., F. Dreyer, and K. Aktories. 1989. Actin involvement in exocytosis from PC12 cells: studies on the influence of botulinum C2 toxin on stimulated noradrenaline release. *J. Neurochem.* 52:370-376.
26. McLaughlin, P. J., J. T. Gooch, H.-G. Mannherz, and A. G. A. Weeds. 1993. Structure of gelsolin segment 1-actin complex and the mechanism of filament severing. *Nature (Lond.).* 364:685-692.
27. Minta, A., J. P. Y. Kao, and R. Y. Tsien. 1989. Fluorescent indicators for cytosolic calcium based on rhodamine and fluorescein chromophores. *J. Biol. Chem.* 264:8171-8178.
28. Muallem, S. 1992. The ins and outs of Ca^{2+} in exocrine cells. *In* Advances in Second Messenger and Phosphoprotein Research: Inositol Phosphates and Calcium Signaling. J. Putney, editor. Raven Press, NY. 351-368.
29. Nachmias, V. T. 1993. Small actin-binding proteins: the β-thymosin family. *Curr. Opin. Cell Biol.* 5:56-62.
30. Norman J. C., L. S. Price, A. J. Ridley, A. Hall, and A. Koffer. 1994. Actin filament organization in activated mast cells is regulated by heterotrimeric and small GTP-binding proteins. *J. Cell Biol.* 126:1005-1015.
31. Nübe O., and M. Lindau. 1988. The dynamics of exocytosis in human neutrophils. *J. Cell Biol.* 107:2117-2123.
32. O'Konski, M. S., and S. J. Pandol. 1990. Effects of caerulein on the apical cytoskeleton of the pancreatic acinar cell. *J. Clin. Invest.* 86:1649-1657.
33. O'Konski, M. S., and S. J. Pandol. 1993. Cholecystokinin JMV-180 and caerulein effects on the pancreatic acinar cell cytoskeleton. *Pancreas.* 8:638-646.
34. Padfield, P. J., W. E. Balch, and J. D. Jamieson. 1992. A synthetic peptide of the rab3a effector domain stimulates amylase release from permeabilized pancreatic acini. *Proc. Natl. Acad. Sci USA.* 89:1656-1660.
35. Pandol, S. J., M. S. Schoeffield, G. Sachs, and S. Muallem. 1985. Role of free cytosolic calcium in secretagogue-stimulated amylase release from dispersed acini from guinea pig pancreas. *J. Biol. Chem.* 260:10081-10086.
36. Popov, S., and M.-M. Poo. 1993. Synaptotagmin: a calcium-sensitive inhibitor of exocytosis? *Cell.* 73:1247-1249.
37. Sanders, M.C, A. L. Goldstein, and Y.-L. Wang. 1992. Thymosin β_4 (Fx peptide) is a peptide regulator of actin polymerization in living cells. *Proc. Natl. Acad. Sci. USA.* 89:4678-4682.
38. Sontag, J.-M., D. Aunis, and M.-F. Bader. 1988. Peripheral actin filaments control calcium-mediated catecholamine release from streptolysin-O-permeabilized chromaffin cells. *Eur. J. Cell Biol.* 46:316-326.

39. Southwick, F. S., and C. L. Young. 1990. The actin released from profilin-actin complexes is insufficient to account for the increase in F-actin in chemoattractant-stimulated polymorphonuclear leukocytes. *J. Cell Biol.* 110:1965–1973.
40. Söllner, T., M. K. Bennett, S. W. Whiteheart, R. H. Scheller, and J. E. Rothman. 1993. A protein assembly-disassembly pathway in vitro that may correspond to sequential steps of synaptic vesicle docking, activation, and fusion. *Cell.* 75:409–418.
41. Söllner, T., S. W. Whiteheart, M. Brunner, H. Erdjument-Bromage, S. Geromanos, P. Tempst, and J. E. Rothman. 1993. SNAP receptors implicated in vesicle targeting and fusion. *Nature (Lond.).* 362:2662–2666.
42. Trifaró, J.-M., A. Rodríguez Del Castillo, and M. L. Vitale. 1992. Dynamic changes in chromaffin cell cytoskeleton as prelude to exocytosis. *Molecular Neurobiology.* 6:339–358.
43. Vitale, M. L., A. Rodrigues del Castillo, L. Tchakarov, and J.-M. Trifaro. 1991. Cortical filamentous actin disassembly and scinderin redistribution during chromaffin cell stimulation precede exocytosis, a phenomenon not exhibited by gelsolin. *J. Cell Biol.* 113:1057–1067.
44. Walent, J. H., B. W. Porter, and T. F. J. Martin. 1992. A novel 145 kd brain cytosolic protein reconstitutes Ca^{2+}-regulated secretion in permeable neuroendocrine cells. *Cell.* 70:765–775.
45. Way, M., J. Gooch, B. Pope, and A. G. Weeds. 1989. Expression of human plasma gelsolin in *Escherichia coli* and dissection of actin binding sites by segmental deletion mutagenesis. *J. Cell Biol.* 109:593–605.
46. Weber, A., V. T. Nachmias, C. R. Pennise, M. Pring, and D. Safer. 1992. Interaction of thymosin β_4 with muscle and platelet actin: implications for actin sequestration in resting platelets. *Biochemistry.* 31:6179–6185.
47. Whitters, E. A., A. E. Cleves, T. P. McGee, H. B. Skinner, and V. A. Bankaitis. 1993. SAC1p is an integral membrane protein that influences the cellular requirement for phospholipid transfer protein function and inositol in yeast. *J. Cell Biol.* 122:79–94.
48. Williams, J. A., and G. T. Blevins. Cholecystokinin and regulation of pancreatic acinar cell function. *Physiol. Rev.* 73:701–723.
49. Yin, H. L. 1987. Gelsolin: calcium- and polyphosphoinositide-regulated actin-modulating protein. *BioEssays.* 7(4):176–178.
50. Yu, F.-X., S.-C. Lin, M. Morrison-Bogorad, and H. L. Yin. 1994. Effects of thymosin β4 and thymosin β10 on actin structures in living cells. *Cell Motil. Cytoskeleton.* 27:13–25.
51. Yu, F.-X., P. A. Johnson, T. C. Sudhof, and H. L. Yin. 1990. gCap39, a calcium ion- and polyphosphoinositide-regulated actin capping protein. *Science (Wash. DC).* 250:1413–1415.
52. Yu, F.-X., S.-C. Lin, M. Morrison-Bogorad, M. A. L. Atkinson, and H. L. Yin. 1993. Thymosin β10 and thymosin β4 are both actin monomer sequestering proteins. *J. Biol. Chem.* 268:502–509.
53. Yu, F.-X., H.-Q. Sun, P. A. Janmey, and H. L. Yin. 1992. Identification of a polyphosphoinositide-binding sequence in an actin monomer-binding domain of gelsolin. *J. Biol. Chem.* 267:14616–14621.
54. Zarbock, J., H. Oschkinat, E. Hannappel, H. Kalbacher, W. Voelter, and T. A. Holak. 1990. Solution conformation of thymosin beta 4: a nuclear magnetic resonance and simulated annealing study. *Biochemistry.* 29: 7814–7821.
55. Zhang, B.-X., H. Zhao, and S. Muallem. 1993. Ca^{2+}-dependent kinase and phosphatase control IP_3-mediated Ca^{2+} release: modification by agonist stimulation. *J. Biol. Chem.* 268:10997–11001.